Evolution of long-range order and composition for radiation-induced precipitate dissolution

Eric Camus, Christian Abromeit, Françoise Bourdeau, Nelja Wanderka, and Heinrich Wollenberger
Hahn-Meitner-Institut Berlin GmbH, Glienicker Strasse 100, D-14109 Berlin, Federal Republic of Germany
(Received 10 November 1995; revised manuscript received 11 April 1996)

Disordering and dissolution of $L1_2$ ordered γ' precipitates under irradiation at temperatures between room temperature and 623 K are investigated by means of transmission electron microscopy and field-ion microscopy with atom probe. The combination of both experimental techniques allows us to follow the disordering process as well as chemical decomposition of the precipitates with atomic resolution. During room-temperature irradiation and for increasing irradiation fluence, the concentration profiles across the precipitates show a broadening of the γ/γ' interface. The experimentally obtained depth profiles can be interpreted assuming a dissolution process of the concentration inhomogeneities due to ballistic transport only. A correlation analysis of the experimental data yields a mixing diffusion coefficient of $D_{\mathrm{mix}}/K=(0.75^{+0.2}_{-0.4})$ nm^2 dpa^{-1}. Depending on irradiation temperature, two dissolution regimes are observed. For a displacement rate of 10^{-3} dpa s^{-1}, the precipitates first disorder and then dissolve in a disordered state at temperatures below 540 K, while disordering and dissolution occur simultaneously at temperatures between 540 and 623 K. These results demonstrate that disordering of the precipitates is not necessarily required for the dissolution. The results are in accordance with recent theoretical predictions for the dissolution mechanism of ordered precipitates under irradiation. [S0163-1829(96)07629-1]

I. INTRODUCTION

Irradiation of alloys by energetic particles may induce substantial microstructural changes and phase transformations. Atomic redistribution of the constituents of an alloy occurs by atomic mixing and by the defect reactions due to the diffusion of the point defects to extended sinks or by recombination. As these reactions are controlled by nonequilibrium processes, they produce a radiation-induced distribution of phases which can differ significantly from that which is expected for thermal treatments.

Heavy-ion irradiation of a two-phase precipitate/matrix microstructure at temperatures where atomic mixing is predominant is known to cause dissolution of the precipitates (for a review, see Ref. 1). The theoretical models developed to describe precipitate stability under irradiation take into account the counteraction of the two processes of dissolution and reprecipitation. The later is generally described by radiation-enhanced growth and coarsening of precipitates. Some differences exist concerning the dissolution process. Nelson, Hudson, and Mazey,[2] and Hudson[3] propose a dissolution model based on a mechanism of recoil dissolution. Precipitate atoms are ejected into the matrix. The evolution of an average precipitate radius is described by a rate equation. The precipitate radius reaches a stationary value depending on irradiation conditions. Abromeit[4] considers the influence of the concentration of point defects on the nucleation process of the precipitates and predicts the existence of a critical radius and of a stationary radius. If the calculated stationary radius is smaller than this critical radius, the precipitates dissolve completely. Frost and Russell[5] model the dissolution by a term of precipitate solute deposition into the matrix, depending on the creation rate of solute recoils and the precipitate size. They treat the precipitate as having a stationary interface. The steady-state value of the matrix solute concentration is calculated and the size evolution of the precipitates is predicted.

When considering the influence of irradiation on a long-range ordered precipitated phase, two aspects are obviously to be considered: (i) dissolution of the precipitated phase and (ii) evolution of the order inside the phase. Both aspects have been addressed in the past experimentally and theoretically.[1,6–9] The dissolution of the precipitates is generally described by resolution due to ballistic effects, which are counteracted by radiation-enhanced diffusion promoting transition back to the thermodynamically stable state. Several models consider either disordering alone[10–12] (evolution of the degree of order under irradiation) or dissolution alone.[4,5,13] Other models describe both processes under different assumptions. Nelson, Hudson, and Mazey[2] and Hudson[3] suppose in their disorder dissolution model that ordered precipitates will dissolve by recoil resolution more effectively than nonordered ones, as creation of disorder will destabilize them. Liou and Wilkes[14] consider that disorder inside of the precipitate induces an increase of free energy which modifies phase diagrams and may cause phase instability.

All these models have the common shortcomings that (i) the influence of the displacement cascades is only considered to change the size of precipitates and (ii) they do not treat the disordering and dissolution as interdependent processes, thus failing to consider details of the thermodynamic relationships in an adequate way. The influence of irradiation on the concentration gradients, precipitate solute atom concentration, and chemical order is not taken into account on a local scale.

Recently, two more elaborate models have been proposed, which overcome these shortcomings and take the local variations of the atomic distribution of the alloy atoms into account. Martin and co-workers[15–22] use a kinetic master equation based on the Bragg-Williams approximation to evaluate

atomic jumps at a discrete scale. The irradiation is modeled by a forcing parameter which characterizes the different kinds of irradiation (electron, light ions or heavy ions). Not only a dissolution of a concentration inhomogeneity, but also transitions between different ordered structures are predicted during the irradiation. These authors treated the dissolution of B_2 ordered as well as of $L1_2$ ordered precipitates in a disordered matrix.

A similar, but simplified approach is taken by Matsumura, Müller, and Abromeit.[23] They use the formalism of Ginzburg-Landau differential equations to describe the spatial and temporal evolutions of the order parameter and species concentrations in a continuum. The details of the ballistic jumps for the change of the concentrations and of the long-range order parameter are neglected. Within this approximation, the evolution of the two-phase structure under irradiation is described by coupled differential equations, which can be solved for various microstructures.[23] As in the more sophisticated treatment of Martin and co-workers[15–22] the symmetry of the precipitate shape is conserved because the cascade effect, which consists of locally and timely correlated bursts of ballistic jumps, is not taken into account. Both approaches[15–23] predict the evolution of the degree of order inside the precipitate and the concentration profile around the precipitate as a function of irradiation parameters and temperature.

In a recent publication, we have reported on disordering at room temperature of the γ' phase as a function of irradiation time by means of transmission electron microscopy (TEM).[24] In this article, we report experimental results on both disordering and dissolution of ordered γ' precipitates as a function of irradiation temperature. Two experimental techniques were used. Field-ion microscopy with atom probe (FIM-AP) is adequate to resolve both the concentration profiles around precipitates and the evolution of concentration gradients adjacent to the interface precipitate/matrix with atomic resolution.[25–27] Disordering of the ordered phase was studied by transmission electron microscopy in the diffraction mode.

In Sec. II we introduce the experimental techniques used in this work. In Sec. III we report results on the dissolution mechanism of the γ' phase of the nickel-base alloy nimonic PE16 at room temperature. Section IV is devoted to coupling of disordering and dissolution at higher temperatures. A discussion of the dissolution mechanism depending on temperature and a comparison with theoretical models are the subject of Sec. V.

II. EXPERIMENTAL TECHNIQUES

A. Field-ion microscopy with atom probe

The field-ion microscopy with atom probe (FIM-AP) is suitable to resolve both the concentration profiles of all species in the precipitate and the evolution of concentration gradients adjacent the interface at a subnanometer scale.[25–27] The principle of the atom-probe technique may be summarized as follows. If a high voltage is applied to a specimen having a small radius of curvature (10 to 100 nm), the field strength at its surface is large enough to eject atoms from the tip surface. This field evaporation process is triggered by a high-voltage pulse. Hence, the chemical identity of the ions can be determined by time-of-flight spectrometry. A circular aperture is installed between the specimen and the single-ion detector and determines the tip area that can be analyzed. The size of this area can be adjusted typically between 1 and 5 nm. During the experiment, the specimen is continuously field evaporated, so that an in-depth analysis of the materials is performed. The depth resolution of the measurement is on the order of one atomic layer. The results of an analysis are the data identifying the successively collected ions. From these raw data, it is possible to deduce quantitative information on the dissolution process, as shown in the next sections.

B. Specimen preparation and irradiation

The alloy nimonic PE16 was chosen for the investigation. It is an Al and Ti containing FeNiCr base alloy. Proper thermal treatment leads to the precipitation of spherical, coherent, $L1_2$ ordered γ' precipitates within a γ matrix. The specimens used in the present investigation were solution annealed at 1313 K for 2 h under argon atmosphere and subsequently aged at 1045 K for 65 min (FIM specimens) or 24 h (TEM specimens) to prepare precipitates of radius 3.5 and 10 nm, respectively. The volume fraction of the γ' phase was 6–7% in both cases, in agreement with published data.[28] This two-phase microstructure constitutes the initial state for all irradiation experiments. The FIM specimens were electropolished in a solution of dilute perchloric acid in order to obtain specimens with a radius of curvature smaller than 50 nm. The specimens were irradiated at the heavy-ion accelerator of the Hahn-Meitner-Institut Berlin. $^{58}Ni^{+}$ ions of 300-keV energy with a flux of 0.8 mA m^{-2} were employed for all experiments. This corresponds to a displacement rate of $K=10^{-3}$ dpa s^{-1} according to the TRIM code calculations.[29] As the penetration depth of such ions is on the order of 100 to 150 nm, the FIM specimens were first prepared, then irradiated, and finally transferred to the field-ion microscope for analysis. More details on the irradiation facility for FIM specimens can be found in Ref. 30. The TEM specimens were thinned electrolytically from one side before irradiation and, after irradiation, back polished from the nonirradiated side until perforation occurred.

III. DISSOLUTION MECHANISM AT ROOM TEMPERATURE

A. FIM-AP depth profiles

A FIM-AP depth profile is obtained by continuous field evaporation of the surface atoms of the specimen and provides the composition of a cylinder of matter. As the field-evaporated ions reach the detector atom by atom, each concentration point in the depth profiles (called a concentration block) is calculated from a given number (typically 50 to 200) of sequentially collected ions. The concentration values obtained this way are plotted as a function of analyzed depth. The analyses were carried out with a diameter of analysis of 1.9 ± 0.2 nm. Such a value is smaller than the average precipitate diameter of approximately 7 nm and allows the detection of roughly 35 atoms per layer in the crystallographic $\langle 111\rangle$ direction. The depth profiles shown in the present article are displayed with concentration blocks containing 100 atoms. This corresponds to approximately 3 atomic layers in the $\langle 111\rangle$ direction.

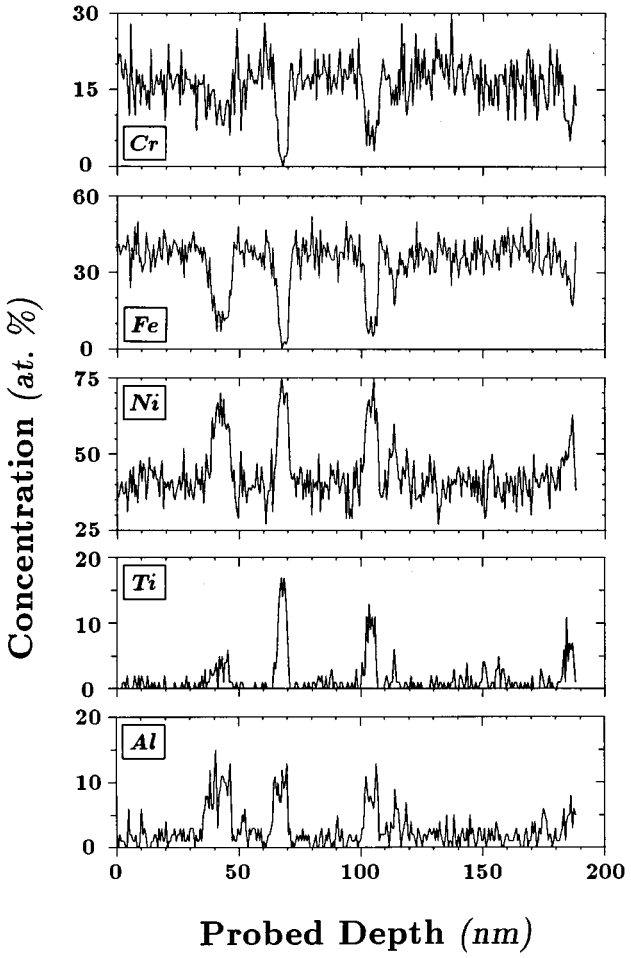

FIG. 1. Concentration depth profiles of a specimen of the alloy nimonic PE16 solution annealed at 1313 K for 2 h, quenched in water, and aged at 1025 K for 65 min. The γ' phase can be easily recognized as a Ni-, Al-, and Ti-rich and Fe- and Cr-depleted phase. Each concentration point in the profiles is calculated from 100 subsequently detected atoms, corresponding to approximately three atomic layers in the direction ⟨111⟩.

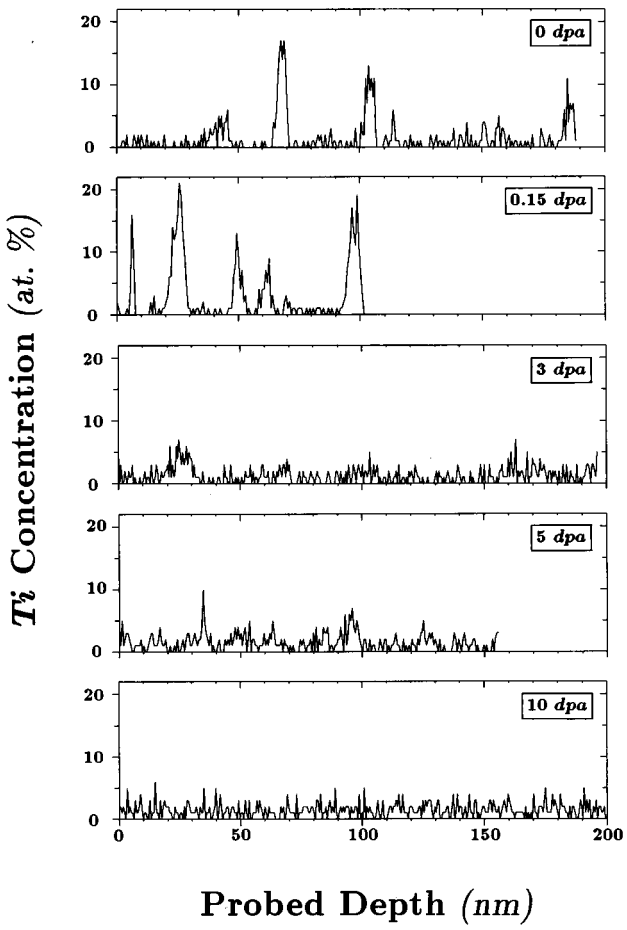

FIG. 2. Ti concentration depth profiles of specimen of the alloy nimonic PE16 irradiated at room temperature to fluences up to 10 dpa with 300-keV Ni^+ at a constant flux of 10^{-3} dpa s^{-1}. The Ti concentration in the γ' precipitates decreases as the fluence increases.

Figure 1 displays the depth profiles of Ni, Fe, Cr, Al, and Ti for a nonirradiated specimen, showing that the γ' precipitates contain a high level of Ni, Al, and Ti, while they are depleted in Fe and Cr. The precipitates have essentially the stoichiometry $Ni_3(Al+Ti)$, which is compatible with the $L1_2$ ordered structure. The aged state corresponding to the profiles shown in Fig. 1 is the initial state before irradiation.

Figure 2 shows the results after irradiation at room temperature on the two-phase mixture. As the ratio of the precipitate concentration to the matrix concentration is approximately 40 in the case of Ti, this element is taken as an indicator to follow the dissolution process. The concentration of all other species are changed accordingly, i.e., the Al and Ni levels in the particles decrease during irradiation, while the Fe and Cr levels increase. We conclude that the γ' particles have dissolved after a fluence of 10 dpa at room temperature.

B. Precipitate/matrix interface

Additional information can be deduced from integrated profiles. In Fig. 3, the cumulative number of Al and Ti ions counted in the detector versus the analyzed depth has been plotted. Two examples are shown, corresponding to the initial state before irradiation and after an irradiation to 5 dpa. In each case, a particle was crossed during analysis. Obviously the dissolution of the particles proceeds by a broadening of the γ/γ' interface.

C. Microstructural parameters

Quantitative information about the dissolution process can be deduced from the depth profiles. The nimonic PE16 alloy contains spherical precipitates. As the measured concentration profile is a projection of the real 3D morphology, it is necessary to apply a correction procedure to deduce size and number density of the precipitates. We have used the geometrical model developed by Blavette and co-workers.[31,32] Assuming the precipitates remain spherical in shape during the dissolution process, it is possible to deduce their number density from the measured concentration profiles. Figure 4 shows the evolution of the number density as a function of fluence at room temperature. It is obvious from this plot that the number density remains constant within experimental error during the dissolution process.

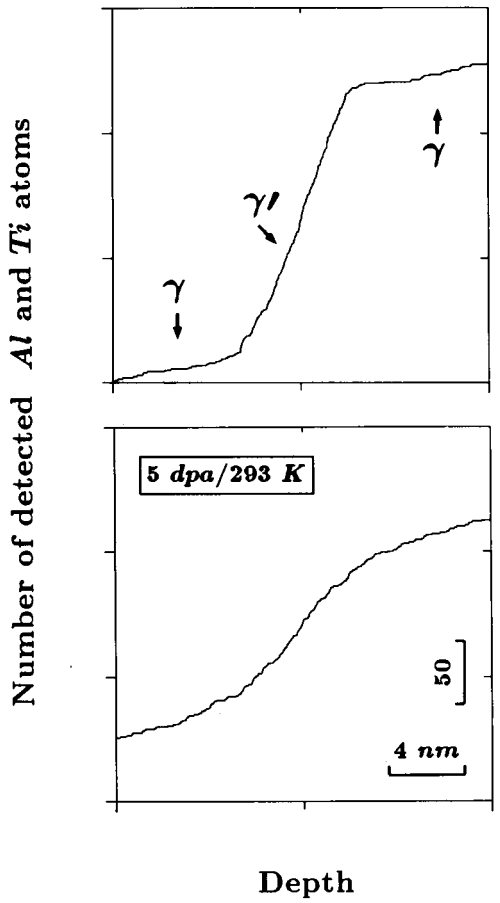

FIG. 3. Total number of detected Al+Ti atoms as a function of the analyzed depth around precipitates before and after irradiation at room temperature to 5 dpa with 300-keV Ni^+ at a constant flux of 10^{-3} dpa s^{-1}. The slopes reveal the different concentrations of Al and Ti in the precipitates and in the matrix. The irradiation results in a broadening of the γ/γ' interface.

A characteristic of the series shown in Fig. 2 is a diminution of the amplitudes of the Ti peaks when the fluence increases. The Ti concentration decreases in the precipitates, while the concentration in the matrix increases. As precipitate radius and diameter of analysis are the same as compared to the nonirradiated state, we conclude that this effect is not due to spatial convolution due to simultaneous analysis of matrix and precipitate.[33]

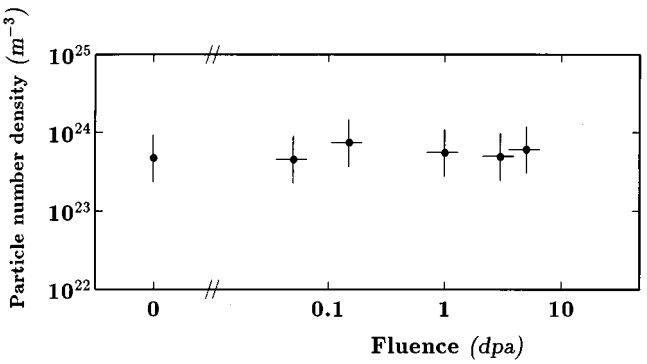

FIG. 4. Evolution of the γ' particle number density as a function of fluence for room-temperature irradiation with 300-keV Ni^+ at a constant flux of 10^{-3} dpa s^{-1}. After 10 dpa, no precipitates were detected in the profiles.

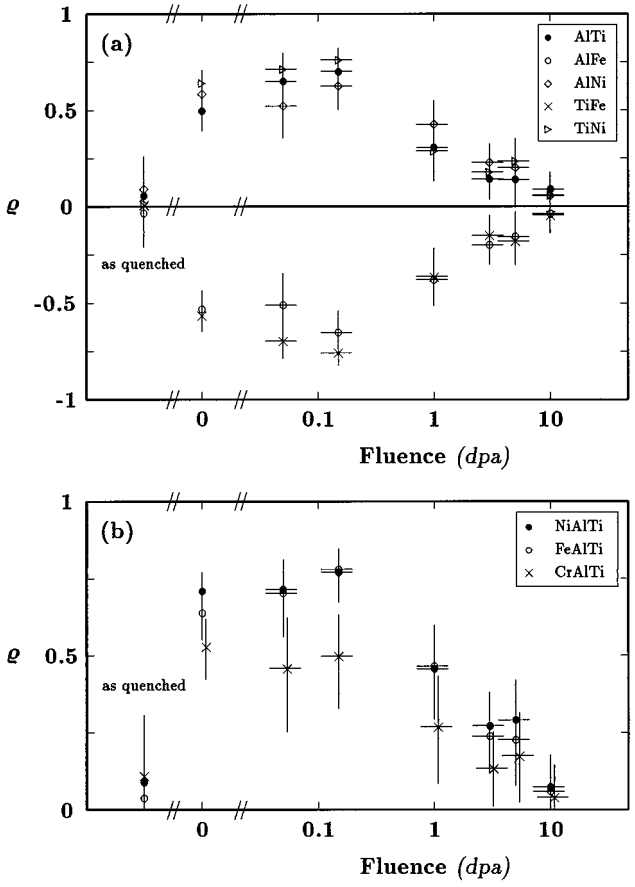

FIG. 5. Evolution of selected correlation coefficients as a function of fluence for room-temperature irradiation with 300-keV Ni^+ at a constant flux of 10^{-3} dpa s^{-1}. The two-element coefficients are positive or negative, indicative of a cosegregation or an antisegregation of the considered elements, respectively. After 10 dpa, all coefficients do not differ significantly from zero, demonstrating that the concentration depth profiles also do not differ significantly from random distributions. The given errors are estimates of the 99.73% confidence interval.

The dissolution process can be quantified by means of an appropriate correlation analysis.[34,35] Indeed, it is obvious from Fig. 1 that, as an example, the variations in composition of the species Ni, Al, and Ti are correlated. The particles are Ni, Al, and Ti rich, while the matrix is Ni, Al, and Ti depleted. The correlation coefficient for the species Ni, Al, and Ti amounts to $\varrho_{\mathrm{NiAlTi}}=0.68\pm0.07$ for the profiles given in Fig. 1. The value of the correlation coefficient is an indicator of the degree of decomposition and depends mainly on the concentration difference between the two phases for the involved species. If the analyzed region is monophase, the depth profiles are at random, and the correlation coefficient is not significantly different from zero. More details concerning the calculation of correlation coefficients from the experimental depth profiles and their significance are given in Refs. 34–36. Figure 5 shows the evolution of some correlation coefficients as a function of the fluence. The given error bars correspond to an estimate of the 99.73% confidence interval.[34] All coefficients decrease in absolute value by in-

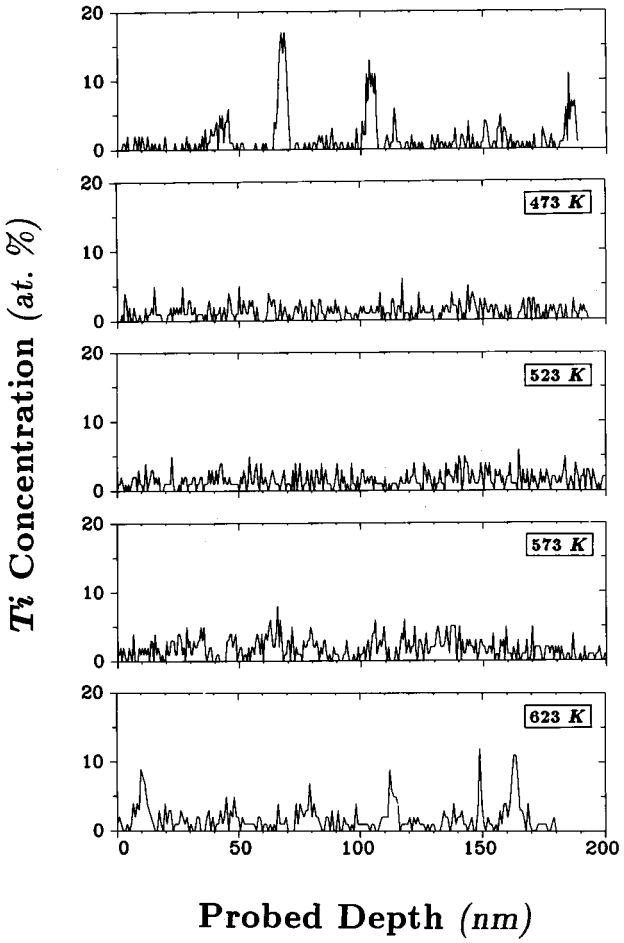

FIG. 6. Ti concentration depth profiles of the γ/γ' alloy nimonic PE16 before irradiation (upper profile) and after irradiation to 10 dpa and at temperatures between 473 and 623 K. In the nonirradiated profiles, the Ti-enriched zones clearly indicate the presence of the γ' phase. Irradiation at the temperatures 473 and 523 K results in dissolution of the γ' precipitates. After irradiation at the temperatures 573 and 623 K, Ti-enriched zones subsist, the Ti content of which is smaller than in the nonirradiated state.

creasing fluence and approach zero after a 10 dpa irradiation. This demonstrates that at 10 dpa the profiles do not differ significantly from random distributions and confirms the idea that the γ' particles are completely dissolved, within the experimental errors due to the employed lateral resolution.[34]

IV. DISSOLUTION AND DISORDERING AT HIGHER TEMPERATURES

The upper profile of Fig. 6 is a FIM-AP concentration depth profile of a nonirradiated specimen for comparison. All other profiles in Fig. 6 are AP analyses of specimens irradiated to 10 dpa at different temperatures. As shown previously, the precipitates dissolve after 10 dpa at room temperature. This holds for temperatures between room temperature and 523 K. At the temperatures of 573 and 623 K, the measured profiles are not yet random. Ti-enriched regions are clearly visible. However, the Ti level in these regions is drastically reduced as compared to the nonirradiated state. The examination of the γ/γ' interface is as previously carried out

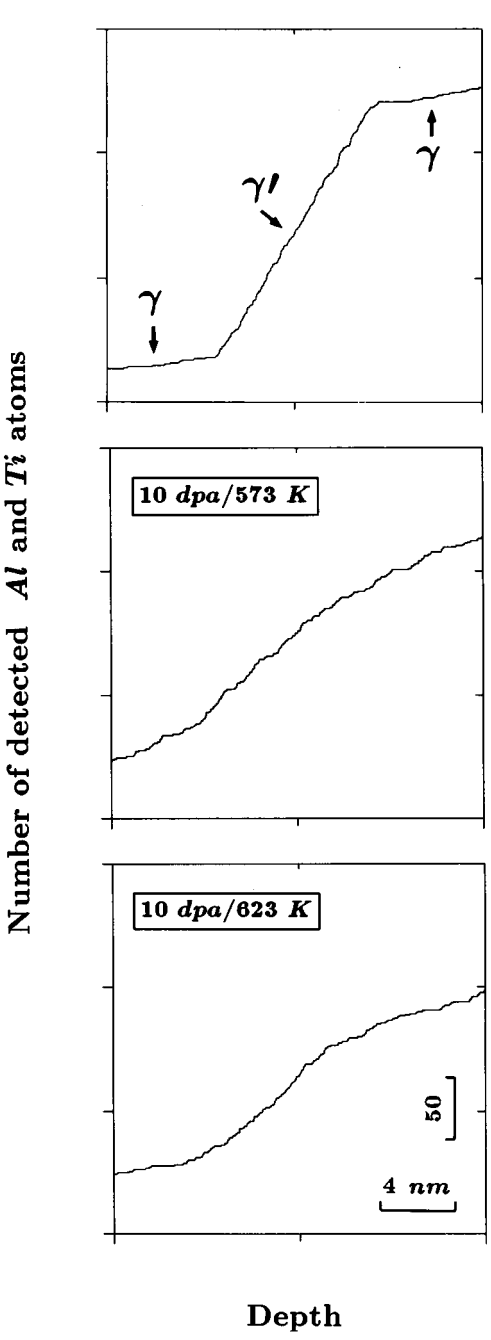

FIG. 7. Total number of detected Al+Ti atoms as a function of the analyzed depth around precipitates. In the nonirradiated state (upper diagram), the different slopes reveal the different concentration of Al+Ti in the matrix and in the γ' precipitates. The γ/γ' transition occurs within approx. 1 atomic layer. After irradiation to 10 dpa at 573 and 623 K, the interface is broadened indicating dissolution of the precipitates.

by plotting the number of detected Al+Ti ions as a function of analyzed depth. The diagrams before irradiation and after irradiations to 10 dpa at 573 and 623 K are displayed in Fig. 7 and show evidence for a broadening of the interface after irradiation. The correlation coefficients $\varrho_{\mathrm{NiAlTi}}$, $\varrho_{\mathrm{FeAlTi}}$, and $\varrho_{\mathrm{CrAlTi}}$ are plotted as a function of irradiation temperature in Fig. 8. The corresponding values before irradiation are given in the inset. It is clear from this picture that (i) in the tem-

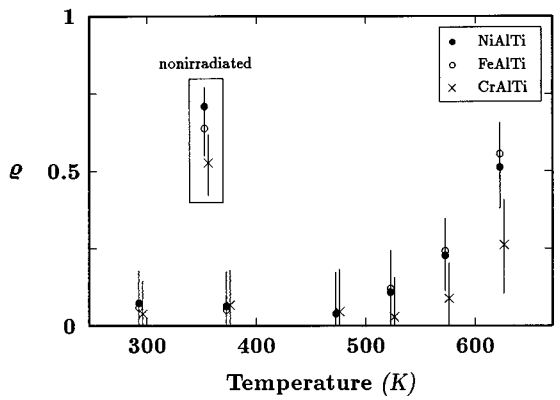

FIG. 8. Correlation coefficients $\varrho_{\mathrm{NiAlTi}}$, $\varrho_{\mathrm{FeAlTi}}$, and $\varrho_{\mathrm{CrAlTi}}$ at a fluence of 10 dpa as a function of the irradiation temperature. At temperatures below 523 K, all coefficients do not differ significantly from zero. The atomic distribution is at random. At the temperatures 573 and 623 K, the coefficients are significantly different from zero but smaller than the respective values of the nonirradiated state, indicating that the dissolution proceeds slower in that temperature region. The given error bars are estimates of the 99.73% confidence interval.

perature range from room temperature to 523 K, where the correlation values are not significantly different from zero, the precipitates dissolve within 10 dpa, and (ii) at the temperatures 573 and 623 K, where the correlation values are reduced as compared to the nonirradiated state, the precipitates dissolve more slowly. Note that at even higher temperatures, the precipitates are expected to undergo radiation-enhanced coarsening.[37]

The disordering process was investigated by TEM by following the intensity of superlattice reflections in zone-axis diffraction patterns. For temperatures between room temperature and 523 K, an irradiation to a fluence of 0.1 dpa causes a drastic diminution of the intensity of the superlattice reflections. At higher fluences, weak superlattice reflections are still visible up to 1 dpa, and disappear after a fluence of 2 to 3 dpa.[12,24] At temperatures above 540 K, the intensity of the superlattice reflections is only slightly reduced after a fluence of 10 dpa. These results, together with those of the FIM investigation, are summarized in Fig. 9. Remember that the initial radius of the precipitates was 3.5 nm for the FIM investigation and 10 nm for the TEM investigation. It results from our observations that, in the temperature range from 540 to 623 K, precipitate dissolution and disordering occur simultaneously.

V. DISCUSSION

From the experimental results, we deduce that at room temperature the dissolution proceeds with (i) constant number density, (ii) variation of the concentration inside of the precipitates, and (iii) broadening of the γ/γ' interface. We conclude that the dissolution of the γ' precipitates is determined by diffusion-controlled transport of the precipitate atoms into the surrounding matrix due to a concentration gradient. The experimental findings of the present study are well reproduced by the Fick's second equation with a constant diffusion coefficient and appropriate boundary conditions, as expected in the case of ballistic mixing.[35,36,38]

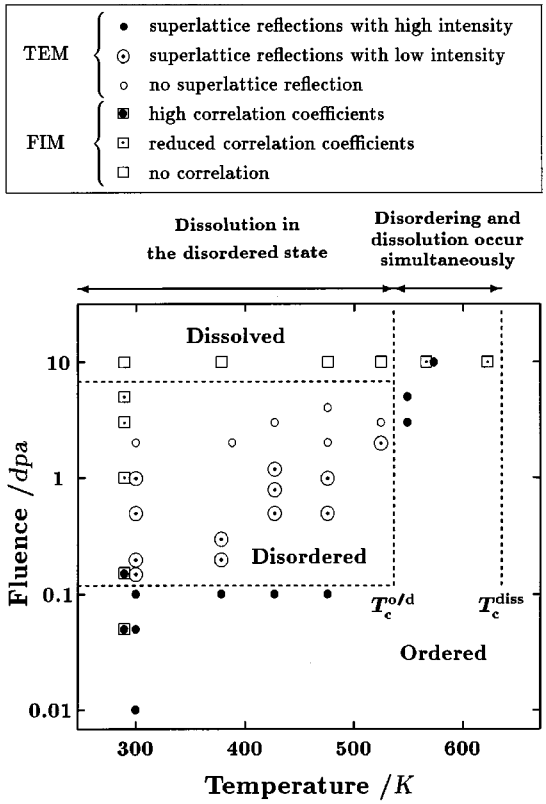

FIG. 9. Disordering and dissolution kinetics of the γ' precipitates under 300 keV Ni^+ irradiation at a displacement rate of 10^{-3} dpa s^{-1}. The diagram shows the combined results obtained on disordering by means of transmission electron microscopy (initial diameter of the precipitates 20 nm) and by field-ion microscopy (initial diameter of the precipitates 7 nm). At temperatures below $T_c^{o/d}\approx 540$ K, the precipitates disorder within 0.1 dpa and dissolve in the disordered state. At temperatures above $T_c^{o/d}$ and below T_c^{diss}, dissolution and disordering occur simultaneously. These two dissolution regimes are in agreement with theoretical predictions.

It is possible to calculate theoretical correlation coefficients corresponding to a given precipitate/matrix geometry.[34,35] We have evaluated the correlation coefficients for the different diffusion profiles in the case of ballistic transport. When assuming that the precipitate mean radius, number density, and composition of both phases are known for the nonirradiated state, a fit of the model calculation[34,35] to the experimental correlation coefficients yields the mixing diffusion coefficient D_{mix}. The results of the theoretical calculation of the coefficients $\varrho_{\mathrm{NiAlTi}}$, $\varrho_{\mathrm{FeAlTi}}$, and $\varrho_{\mathrm{CrAlTi}}$ are shown in Fig. 10 together with the coefficients calculated from the experimental profiles. The calculated and measured coefficients agree very well within estimated errors. We deduce the value

$$D_{\mathrm{mix}}=(7.5^{+2}_{-4})10^{-22}\ \mathrm{m^2\,s^{-1}},$$

i.e., for the ratio

$$\frac{D_{\mathrm{mix}}}{K}=(0.75^{+0.2}_{-0.4})\ \mathrm{nm^2\,dpa^{-1}}.$$

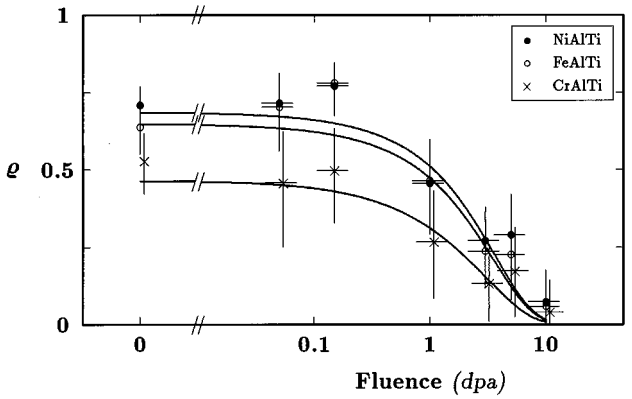

FIG. 10. Fluence dependence of selected correlation coefficients. Comparison of the theoretical coefficients (solid lines), calculated by supposing the particles dissolve via the mechanism proposed in this publication, with the experimental coefficients yields a value of $D_{\mathrm{mix}}/K=(0.75^{+0.2}_{-0.4})$ nm^2 dpa^{-1} for the mixing diffusion coefficient at room temperature.

Diffusion measurements on thin layers by means of secondary ion-mass spectrometry[39–41] (SIMS) have shown that the diffusion profiles obtained after room-temperature irradiation can be interpreted in terms of a phenomenological diffusion coefficient D_{mix}. Table I contains values of the ratio D_{mix}/K for different alloys, all measured under irradiation with Ni^+ ions of 300-keV energy. These values are in reasonable agreement with the value measured in the present work. From the value $D_{\mathrm{mix}}/K=0.75$ nm^2 dpa^{-1} the number of replacements per displacement $n_r/n_d=70$ is obtained. This number is in accordance with the assumption that the dissolution of the precipitates is due to the displacement cascades.[6] We conclude that the kinetics of dissolution is governed by the ballistic process which is imposed by the displacement cascades. The initial state of long-range order of the precipitates plays a minor role. This rules out the idea of Nelson that the dissolution at low temperatures of initially ordered precipitates is more effective than that of nonordered ones.[2]

The models of Nelson,[2] Hudson,[3] and Abromeit[4] describe the effect of the irradiation by superposing the processes of cascade dissolution and radiation-enhanced reprecipitation. A basic assumption of these models is dissolution only via a reduction of precipitate radius, without calculating the changes in composition. Frost and Russell[5] treat the particles as having a stationary interface. In contrast, we have shown in the present work that the dissolution proceeds through chemical decomposition of the γ' precipitates, i.e., a drastic change of their composition. Hence, the theoretical models cited above do not describe details of the dissolution process during irradiation at lower temperatures.

TABLE I. Experimental values of the ratio D_{mix}/K obtained under irradiation with Ni^+ ions of 300-keV energy.

Alloy	D_{mix}/K	Source
$Cu_{45}Ni_{47}Fe_8$	2.2 nm^2 dpa^{-1}	Ref. 30
$Fe_{60}Ni_{20}Cr_{20}$	1.6 nm^2 dpa^{-1}	Ref. 39
$Fe_{20}Ni_{60}Cr_{20}$	0.9 nm^2 dpa^{-1}	Ref. 39
Ni	1.2 nm^2 dpa^{-1}	Ref. 41
Cu	0.9 nm^2 dpa^{-1}	Ref. 41
Nimonic PE16	0.75 nm^2 dpa^{-1}	Present investigation

The present experimental results, however, are well described by the recently developed theoretical descriptions by Martin and co-workers[15–22] and Matsumura, Müller, and Abromeit.[23] As local irregularities of the shape of the concentration profiles could not be resolved by the applied experimental technique, the basic approximation of statistically distributed jumps induced by atomic replacements is an adequate assumption. The concentration profiles determined at room temperature are the result of a diffusion-controlled dissolution process with a constant diffusion coefficient. No influence of thermodynamic forces which would lead to jump directions according to the gradient of the chemical potential is found at room temperature.

TEM results concerning room-temperature disordering of the γ' have been reported in a recent publication.[24] The disordering process was followed in the diffraction mode by following the decrease in intensity of the superlattice reflections. The initial radius of the γ' precipitates was 10 nm. For the same irradiation conditions as in the present study, a considerable diminution of the intensity of the superlattice reflections is observed after a fluence of 0.1 dpa. For fluences between 0.1 and 1 dpa, a residual intensity is observed. This intensity disappears after an irradiation of 2 to 3 dpa. This behavior is explained by supposing the precipitates to reach a nonzero stationary value of the long-range order parameter[12] and dissolve via the mechanism proposed in the present study.

The present experimental results allow us to give a detailed picture of the dissolution process of the ordered γ' precipitates. There is clear evidence that *two different dissolution regimes* are occuring at different temperatures.

At temperatures below $T_c^{o/d}\approx 540$ K, the precipitates first disorder and then dissolve. In an intermediate temperature interval, 540 K$<T<$623 K disordering and dissolution occur simultaneously. In other words, disordering of the precipitates *is not a preliminary condition to their dissolution.*

The two dissolution regimes observed experimentally in the present study are also reproduced by the theoretical models of Martin and co-workers[15–22] on both B_2 and $L1_2$ structures and Matsumura, Müller, and Abromeit[23] with a continuum description: depending on irradiation flux and temperature, the precipitates dissolve either in a disordered state, or dissolution and disordering occur simultaneously.

The shapes of the diffusion profiles around a precipitate during the dissolution process at low and high temperature must be different. At low temperature, the precipitates dissolve via a ballistic interdiffusion process. Supposing this type of profile to be valid at higher temperature, the remaining fraction of ordered γ' phase would be too small to explain the observed intensity of the superlattice reflections. We conclude that the precipitate region within the composition range of the γ' phase must be broader, the interface at this high temperature being, however, not as sharp as that of the nonirradiated one. The precipitate dissolution consists of a shrinkage of the precipitate size and a corresponding change of the solute concentration profile at the front of the interface. Typical shapes of calculated diffusion profiles cor-

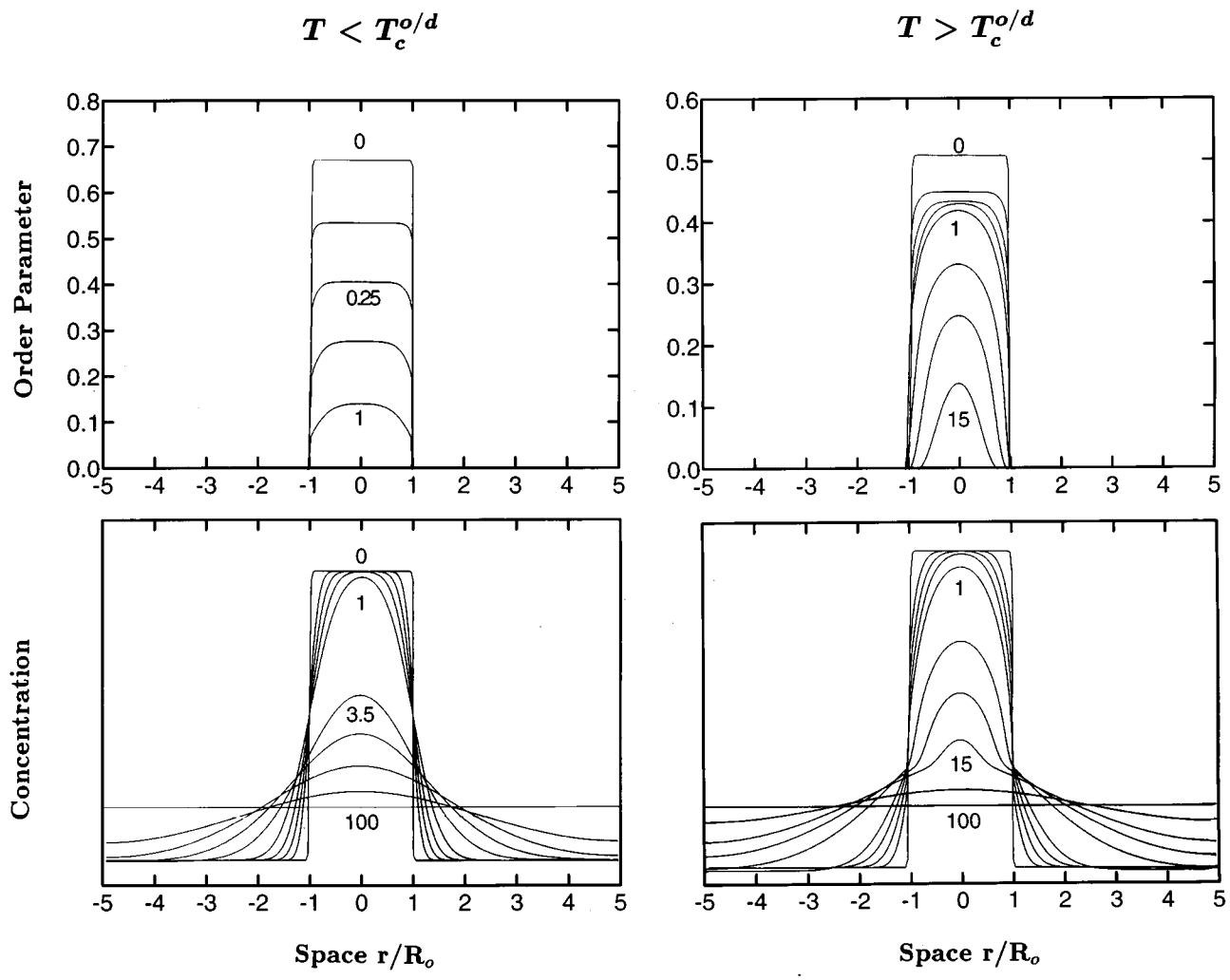

FIG. 11. Dissolution process of an ordered precipitate under irradiation (Ref. 23). Before irradiation, the interface is steplike at $r/R_0 = \pm 1$. R_0 is the initial precipitate radius. During irradiation below $T_c^{o/d}$, the precipitates first disorder and dissolve by ballistic mixing only. At temperatures above $T_c^{o/d}$, disordering and dissolution occur simultaneously. The given numbers at the curves are relative time units.

responding to the two dissolution regimes[23] are shown in Fig. 11. A more detailed analysis of the calculated profiles by correlation analysis is expected to give a more quantitative picture of the dissolution process.[34,35,42]

VI. CONCLUSION

We have presented an experimental investigation of the dissolution mechanism of γ' precipitates under cascade producing irradiation. The main conclusions can be summarized as follows.

(i) The precipitates dissolve via a ballistic interdiffusion process which can be described phenomenologically by a diffusion coefficient D_{mix}. The kinetics of dissolution was determined quantitatively by an appropriate analysis of the depth profiles. The radiation-induced diffusion coefficient normalized by the displacement rate amounts to $D_{\mathrm{mix}}/K = 0.75\ \mathrm{nm}^2\ \mathrm{dpa}^{-1}$.

(ii) Two dissolution regimes are observed. At such temperatures where ballistic jumps are dominant for atomic redistribution, the long-range order is destroyed very efficiently before a significant destruction of the precipitate/matrix interface can be observed. The precipitates are first disordered and then dissolved. At higher temperatures, the dissolution process is slowed down and reordering is increased. Disordering and dissolution occur simultaneously.

(iii) These experimental findings are in agreement with recent model calculations based on Bragg-Williams or time-dependent Ginzburg-Landau approximations.

ACKNOWLEDGMENTS

This work was supported in part within the French-German exchange program Procope. We are grateful to Dr. Georges Martin for his encouragement and many helpful discussions during the whole course of this work. Many thanks are due to Dr. Volkmar Naundorf for valuable comments on the manuscript. We are particularly indebted to the Saclay group, France, especially Dr. Pascal Bellon and Dr. Frédéric Soisson, and to Dr. Shō Matsumura, Kyūshū University, Fukuoka, Japan, for providing us with unpublished results.

[1] K. C. Russell, Mater. Sci. Eng. **28**, 229 (1984).
[2] R. S. Nelson, J. A. Hudson, and D. J. Mazey, J. Nucl. Mater. **44**, 318 (1972).
[3] J. A. Hudson, J. Br. Nucl. Energy Soc. **14(2)**, 127 (1975).
[4] C. Abromeit, in *Irradiation Behaviour of Metallic Materials for Fast Reactor Core Component*, edited by J. Poirier and J.-M. Dupouy (CEA-DMECN, Gif-sur-Yvette, 1979), p. 89.
[5] H. J. Frost and K. C. Russell, Acta Metall. **30**, 953 (1982).
[6] H. Wollenberger, Nucl. Instrum. Methods Phys. Res. Sect. B **48**, 493 (1990).
[7] H. Wollenberger, Mater. Sci. Forum **97–99**, 241 (1992).
[8] H. Wollenberger, in *Metastable Microstructures: Principles, Design and Applications*, edited by D. Banerjee and L. A. Jacobson (Oxford & IBH, New Delhi, 1993), p. 149.
[9] K. C. Russell, J. Nucl. Mater. **206**, 129 (1993).
[10] R. H. Zee and P. Wilkes, Philos. Mag. A **42**, 463 (1980).
[11] S. Banerjee and K. Urban, Phys. Status Solidi A **81**, 145 (1984).
[12] C. Abromeit and H. Wollenberger, J. Nucl. Mater. **191–194**, 1092 (1992).
[13] A. A. Turkin, A. S. Bakai, and A. V. Buts, Mater. Sci. Forum **97–99**, 343 (1992).
[14] K.-Y. Liou and P. Wilkes, J. Nucl. Mater. **87**, 317 (1979).
[15] E. Salomons, P. Bellon, F. Soisson, and G. Martin, Phys. Rev. B **45**, 4582 (1992).
[16] F. Soisson, P. Bellon, and G. Martin, Phys. Rev. B **46**, 11 332 (1992).
[17] F. Soisson, Ph.D. thesis, Institut National Polytechnique de Grenoble, 1993.
[18] G. Martin, F. Soisson, and P. Bellon, J. Nucl. Mater. **205**, 301 (1993).
[19] P. Bellon, F. Soisson, and G. Martin, J. Phys. (France) IV, Colloq. C7, suppl. J. Phys. (France) III **3**, 1977 (1993).
[20] F. Soisson, P. Bellon, and G. Martin, J. Phys. (France) IV, Colloq. C3, suppl. J. Phys. (France) III **4**, 183 (1994).
[21] G. Martin and P. Bellon, in *Statics and Dynamics of Alloy Phase Transformation*, edited by P. A. E. Turchi and A. Gonis (Plenum, New York, 1994), p. 605.
[22] P. Bellon, Y. Grandjean, M. Przybylowicz, F. Soisson, and G. Martin, Nucl. Instrum. Methods Phys. Res. Sect. B **102**, 72 (1995).
[23] S. Matsumura, S. Müller, and C. Abromeit, Phys. Rev. B (to be published).
[24] F. Bourdeau, E. Camus, C. Abromeit, and H. Wollenberger, Phys. Rev. B **50**, 16 205 (1994).
[25] R. Wagner, *Field Ion Microscopy* (Springer, Berlin, 1982).
[26] M. K. Miller and G. D. W. Smith, *Atom-Probe Microanalysis: Principles and Applications to Materials Problems* (Materials Research Society, Pittsburgh, 1989).
[27] T. Sakurai, A. Sakai, and H. W. Pickering, *Atom-Probe Field Ion Microscopy and Its Applications* (Academic, New York, 1989).
[28] H. P. Degischer, W. Hein, H. Strecker, and R. P. Wahi, Z. Metallkd. **78**, 237 (1987).
[29] J. P. Biersack and L. G. Haggmark, Nucl. Instrum. Methods **174**, 257 (1980).
[30] R. Lang, W. Wagner, and H. Wollenberger, J. Nucl. Mater. **175**, 5 (1990).
[31] D. Blavette and S. Chambreland, J. Phys. (Paris) Colloq. **47**, C7-11, 503 (1986).
[32] D. Blavette, A. Menand, and A. Bostel, J. Phys. (Paris) Colloq. **48**, C6-11, 571 (1987).
[33] D. Blavette, Surf. Sci. **266**, 299 (1992).
[34] E. Camus and C. Abromeit, J. Appl. Phys. **75** (5), 2373 (1994).
[35] E. Camus and C. Abromeit, Z. Metallkd. **85**, 378 (1994).
[36] E. Camus, Fortschritt-Bericht-VDI 310 (VDI-Verlag, Düsseldorf, 1993), Series 5.
[37] D. I. Potter, Defect Diff. Forum **61**, 13 (1988).
[38] J. Crank, *The Mathematics of Diffusion* (Clarendon, Oxford, 1975).
[39] A. Müller, Ph.D. thesis, T. U. Berlin, 1987.
[40] A. Müller, V. Naundorf, and M.-P. Macht, J. Appl. Phys. **64**, 3445 (1988).
[41] A. Müller, M.-P. Macht, and V. Naundorf, J. Nucl. Mater. **179–181**, 958 (1991).
[42] C. Abromeit, E. Camus, and S. Matsumura (unpublished).